

An overview of heavy quark energy loss puzzle at RHIC

Magdalena Djordjevic

Dept. Physics, Ohio State University, 191 West Woodruff Avenue, Columbus, OH 43210, USA

August 30, 2018

Abstract

We give a theoretical overview of the heavy quark tomography puzzle posed by recent non-photon single electron data from central Au+Au collisions at $\sqrt{s} = 200$ AGeV. We show that radiative energy loss mechanisms alone are not able to explain large single electron suppression data, as long as realistic parameter values are assumed. We argue that combined collisional and radiative pQCD approach can solve a substantial part of the non-photon single electron puzzle.

1 Introduction

Quark Gluon Plasma (QGP) is a new form of matter, consisting of interacting quarks, antiquarks and gluons. If the QGP can be created in Ultrarelativistic Heavy Ion Collisions (URHIC), then a wide variety of probes and observables could be used to diagnose and map out its physical properties.

Measured quenching patterns of pions and η mesons [1] already provided a direct evidence for the creation of a strongly interacting Quark Gluon Plasma (sQGP) in central Au+Au collisions at $\sqrt{s} = 200$ AGeV [2]-[5]. Further, rare heavy quark jets are considered to be excellent independent probes of the sQGP [6], because their high mass ($m_c \approx 1.2$ GeV, $m_b \approx 4.75$ GeV) changes the sensitivity of the energy loss mechanisms in a well defined way [7]-[12] relative to those of light quark and gluon jets [2]-[4]. Another advantage of heavy quarks jet quenching is that gluon jet fragmentation into heavy mesons can be safely neglected. However, one disadvantage of heavy meson tomography is that direct measurements of identified high p_{\perp} D and B mesons are very difficult with current detectors and RHIC luminosities [13]. Therefore, the first experimental studies of heavy quark attenuation at RHIC have focused on the attenuation of their single (non-photon) electron decay products [14, 15].

The first preliminary data [14, 15] surprisingly suggest that single electrons with $p_{\perp} \sim 5$ GeV may experience elliptic flow and suppression patterns similar to light hadrons. It was measured that the suppression of non-photon electrons, which is expressed in terms of the nuclear modification factor $R_{AA}^e(p_{\perp}) = dN(AA \rightarrow e)/(N_{AA}^{bin} dN(pp \rightarrow e))$, reaches a value $\sim 0.1 - 0.4$ at $p_{\perp} \sim 4 - 8$ GeV. Significant reduction at high p_{\perp} single electrons suggests sizeable heavy quark energy loss.

Motivated by these data, in [16] we applied the theory of heavy quark radiative energy loss [7]-[12] to predict the quenching pattern of single electrons from the decay of high p_{\perp} open charm and bottom hadrons. We showed that because the heavy quark “dead cone” effect [7] is large - especially for bottom quarks - radiative energy loss predictions for R_{AuAu}^e are significantly above 0.5 as long as realistic parameter values are used. Therefore, the puzzle raised by the non-photon single electron data is whether these data can be explained by the energy loss mechanisms in QGP?

This proceeding mainly concentrate on a theoretical overview of the heavy quark energy loss puzzle posed by the single electron data. We start the proceedings with a brief overview of heavy quark production and radiative heavy quark energy loss mechanisms in QGP. We then study the bottom contribution to the single electron spectra, and show that this contribution is significant, and

can not be neglected in the computation of single electron suppression. We then compute the single electron suppression from the radiative energy loss mechanisms, and show that radiative energy loss alone leads to a disagreement with the single electron data, as long as realistic gluon rapidity density is taken into account. Finally, we concentrate on the collisional energy loss, and show that the inclusion of this additional mechanism may lead to a better agreement with the single electron data.

2 Single electron suppression from radiative energy loss

In this section we will compute the single electron suppression which comes from the radiative energy loss mechanisms, and show that the prediction significantly underestimate the single electron suppression as long as realistic values of gluon rapidity density are used.

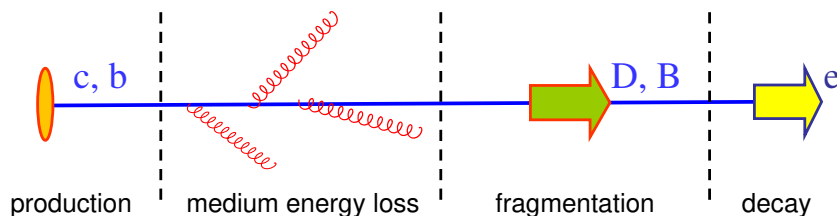


Figure 1: A simplified scheme showing how are the non-photonc single electrons obtained from QGP.

To compute the single electron suppression, we start from Fig. 1, which shows the simplified scheme of how the non-photonc single electrons are obtained from QGP. We see that, in order to compute the single electron spectra, we need to know the initial heavy quark distributions from perturbative QCD, heavy flavor energy loss, heavy quark fragmentation into heavy hadrons, H_Q , and H_Q decay into leptons. The cross section is schematically written as (see [16, 17]):

$$\frac{E d^3 \sigma(e)}{dp^3} = \frac{E_i d^3 \sigma(Q)}{dp_i^3} \otimes P(E_i \rightarrow E_f) \otimes D(Q \rightarrow H_Q) \otimes f(H_Q \rightarrow e),$$

where \otimes is a generic convolution. The electron decay spectrum, $f(H_Q \rightarrow e)$, includes the branching ratio to electrons. The change in the initial heavy flavor spectra due to energy loss is denoted $P(E_i \rightarrow E_f)$.

2.1 Initial heavy quark p_\perp distributions

One of the main advantages of heavy quarks is their large mass (i.e. $M_Q \gg \Lambda_{QCD}$), which, in principle, makes perturbative calculations of heavy quark production possible.

An extensive study of perturbative heavy quark p_\perp distributions can be found in the following papers [19, 20] and references therein. By using these papers we can perturbatively compute and compare the charm and bottom p_\perp distributions. To compute the initial heavy quark p_\perp distributions in central rapidity region ($|y| < 0.5$) we used the MNR code [20]. We assume the same mass and factorization scales as in Ref. [21], that is we use $M_c = 1.2$ GeV ($M_b = 4.75$ GeV) for charm (bottom) mass. For simplicity, we have concentrated only on bare quark distributions ($\langle k_\perp^2 \rangle = 0$ GeV²), and the runs were performed by using CTEQ5M parton distributions. Initial p_\perp distributions used in our computations are shown on the left panel of Fig. 2. From the left panel of Fig. 2 we see that at low momentum region, bottom contribution is negligible compared to charm contribution. On the other hand, at higher momentum region these two contributions become approximately the same. This is a first indication that bottom contribution may become important in the single electron spectrum.

2.2 Radiative heavy quark energy loss

There are three medium effects that control heavy quark radiative energy loss. These effects are 1) Ter-Mikayelian, or massive gluon effect [9, 22], 2) Transition radiation [23, 24] which comes from the fact that medium has finite size and 3) Medium induced radiative energy loss [8], which corresponds to the additional gluon radiation induced by the interaction of the jet with the medium. In [10] we showed that first two effects are not important for the heavy quark suppression, since they lead to a change of ± 0.1 in the charm and bottom R_{AA} . We therefore neglect these two effects in this proceedings, and concentrate only on the medium induced gluon radiation spectrum, given by:

$$\frac{dN_{ind}^{(1)}}{dx} = \frac{C_F \alpha_S}{\pi} \frac{L}{\lambda_g} \int_0^\infty \frac{2\mathbf{q}^2 \mu^2 d\mathbf{q}^2}{\left(\frac{4Ex}{L}\right)^2 + (\mathbf{q}^2 + M^2 x^2 + m_{g,p}^2)^2} \int \frac{d\mathbf{k}^2 \theta(2x(1-x)p_\perp - |\mathbf{k}|)}{((|\mathbf{k}| - |\mathbf{q}|)^2 + \mu^2)^{3/2} ((|\mathbf{k}| + |\mathbf{q}|)^2 + \mu^2)^{3/2}} \times \left\{ \mu^2 + (\mathbf{k}^2 - \mathbf{q}^2) \frac{\mathbf{k}^2 - M^2 x^2 - m_{g,p}^2}{\mathbf{k}^2 + M^2 x^2 + m_{g,p}^2} \right\}. \quad (1)$$

Here, \mathbf{k} is the transverse momentum of the radiated gluon and \mathbf{q} is the momentum transfer to the jet. M is heavy quark mass, $\mu \approx 0.5$ GeV is Debye mass, $\lambda_g \approx 1$ fm is the mean free path, $L \approx 5$ fm is assumed thickness of the medium, $m_{g,p} = \mu/\sqrt{2}$ [9] is gluon mass in the medium, $m_{g,v} \approx \Lambda_{QCD}$ is gluon mass in the vacuum and $E = \sqrt{p_\perp^2 + M^2}$ is initial heavy quark energy. We assume constant $\alpha_S = 0.3$ in this study.

2.3 Heavy quark p_\perp distributions before and after quenching

By knowing the initial heavy quark p_\perp distributions and the heavy quark radiation spectrum, we are able to compute the heavy flavor p_\perp distributions after quenching. For this purpose, we generalized the multigluon fluctuation approach from [3] to the case of finite mass. We here give only the final results, while for more details the reader should refer to [10, 16, 17].

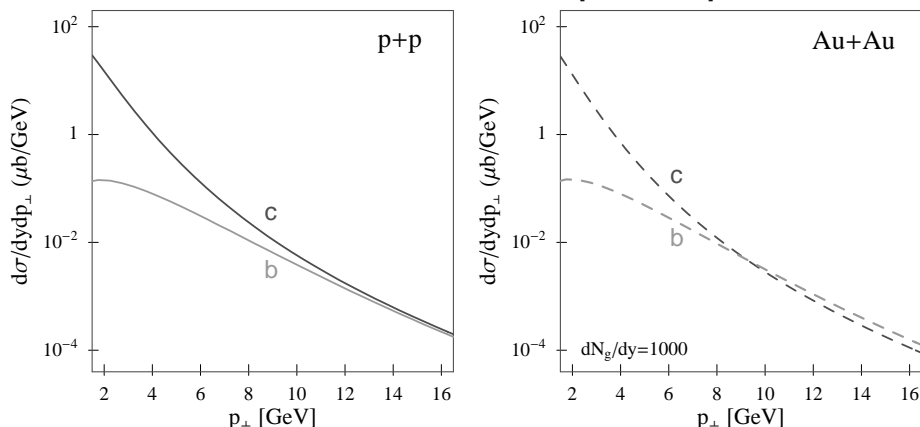


Figure 2: Heavy quark p_\perp distributions before and after quenching are shown on the left and right panels respectively. For the right panel, assumed gluon rapidity density is $dN_g/dy = 1000$ [5, 18]. Dark (light) gray curves correspond to charm (bottom) quarks.

Figure 2 compare p_\perp distributions for heavy quarks before and after quenching. We see that, while before quenching ($p+p$ collisions) charm p_\perp distribution is always larger than bottom p_\perp distribution, after quenching ($Au + Au$ collisions) bottom p_\perp distribution starts to dominate the spectra after ~ 9 GeV. This is expected, having in mind that bottom loose significantly less energy than charm quark (compare dot-dashed curves in Fig. 6), and it is therefore less suppressed than charm quark.

2.4 Radiative energy loss prediction for single electron suppression

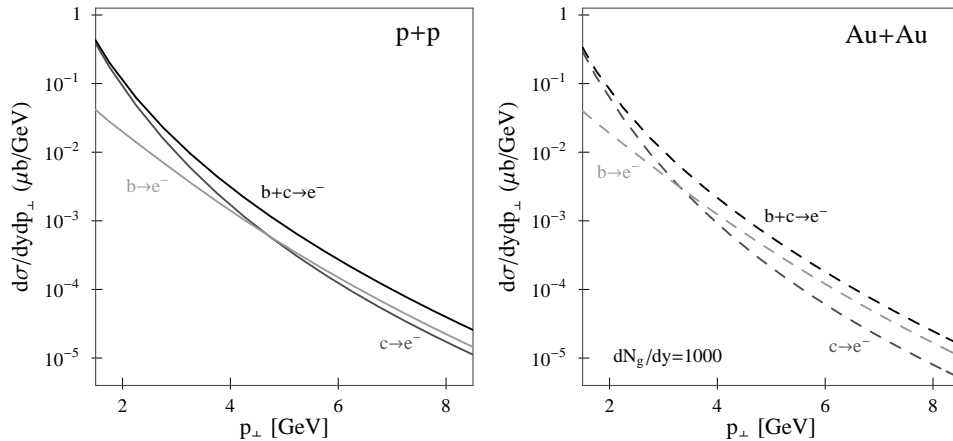


Figure 3: Single electron p_{\perp} distributions before and after quenching are shown on the left and right panels respectively. For the right panel, assumed gluon rapidity density is $dN_g/dy = 1000$. Dark (light) gray curves correspond to charm (bottom) quark contribution to single electrons. Black curves show total (charm and bottom) single electron p_{\perp} distributions.

In this subsection we show the single electron p_{\perp} distributions before and after quenching, which are obtained after fragmentation and decay of heavy quark p_{\perp} distributions from the previous subsection. For more details on how we obtained these p_{\perp} distributions, the reader should refer to [16, 19].

Figure 3 compare p_{\perp} distributions for single electrons before and after quenching. We see that, in the case when quarks are not quenched, bottom contribution to single electron spectrum becomes comparable to charm contribution at $p_{\perp} \sim 5.5$ GeV. For $dN_g/dy = 1000$ case, the crossover between charm and bottom contribution is reduced to $p_{\perp} \sim 3.5$ GeV. Therefore, in QGP, electrons in the $p_{\perp} \sim 5$ GeV region have to be sensitive to both b and c quark quenching.

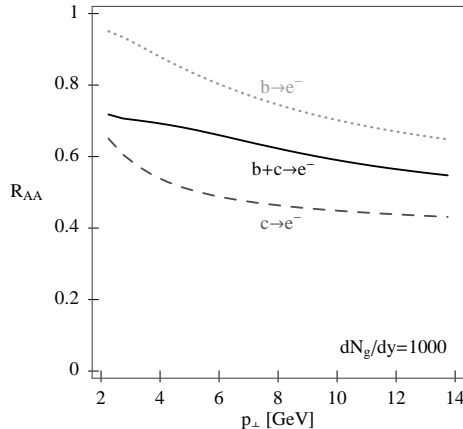


Figure 4: Radiative energy loss prediction for single electron suppression. Assumed initial gluon rapidity density is $dN_g/dy = 1000$. Dashed (dotted) curve shows what would be the single electron suppression if single electrons would have only charm (bottom) contribution. Full curve shows the non-photonc single electron suppression by taking into account both charm and bottom quark contributions.

We can now divide p_{\perp} distributions before and after quenching to obtain the single electron suppression that comes from radiative energy loss computations (see Fig. 4). We see that, for realistic values of gluon rapidity density, radiative energy loss predicts small single electron $R_{AA} \approx 0.7 \pm 0.1$, which is in disagreement with RHIC single electron data [14, 15]. One possible solution to this problem

is to enhance the gluon rapidity density to a maximal value, which would still fit the lower boundary on pion suppression data. In [16], we showed that for $dN_g/dy \sim 3500$ the non-photon single electrons can be suppressed to $R_{AA} \sim 0.5 \pm 0.1$. However, such large values of gluon rapidity density would violate the bulk entropy bounds. Similarly, in Ref. [12], it was found that a similarly excessive transport coefficient [25], $\hat{q}_{eff} \sim 14 \text{ GeV}^2/\text{fm}$, was necessary to approach the measured suppression of electrons from charm jet decay. This finding raised the question of what is the cause for the observed discrepancy between theoretical predictions and experimental results.

3 Collisional energy loss as a solution to the problem?

Recent studies [26, 27] suggested that one of the basic assumptions that pQCD collisional energy loss is negligible compared to radiative [28] may be incorrect. In [26, 27] it was shown that, for a range of parameters relevant for RHIC, radiative and collisional energy losses for heavy quarks were in fact comparable to each other, and therefore collisional energy loss can not be neglected in the computation of jet quenching. This result came as a surprise because from the earlier estimates [28]-[31], the typical collisional energy loss was erroneously considered to be small compared to the radiative energy loss.

However, the computations [26]-[31] were done in an infinite QCD medium, while the medium created in URHIC has finite size. A recent paper by Peigne *et al.* [32] is the first study that made an attempt to include finite size effects in the collisional energy loss. This work suggested that collisional energy loss is large only in an ideal infinite medium case¹, while finite size effects lead to a significant reduction of the collisional energy loss. However, this paper did not completely separate collisional and radiative energy loss effects. Consequently, it remained unclear how important are the finite size effects on the collisional energy loss.

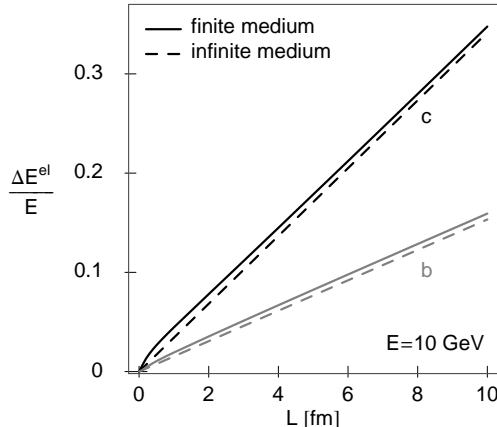


Figure 5: Fractional collisional energy loss is shown as a function of thickness of the medium for charm and bottom quark jets (upper and lower set of curves respectively). Full curves correspond to finite medium case, while dash-dotted curves correspond to infinite medium case. Initial momentum of the jet is 10 GeV. We assume constant $\alpha_S = 0.3$.

Therefore, it became necessary to consistently compute (only) the collisional energy loss in a finite size QCD medium, and see whether the collisional energy loss should be taken into account in the computation of jet quenching. In [33] we provided a detailed study of the 0th order collisional energy loss in a finite size QCD medium created in URHIC. Contrary to [32], we find that a finite size medium does not have a large effect on the collisional energy loss, as shown in Fig. 5.

¹In the case of an infinite QCD medium, the collisional energy loss per unit length dE_{el}/dL is computed by assuming that the jet is produced at $x_0 = \infty$. The energy loss for a finite size medium is then (simplistically) calculated by multiplying this dE_{el}/dL with the thickness L of the medium.

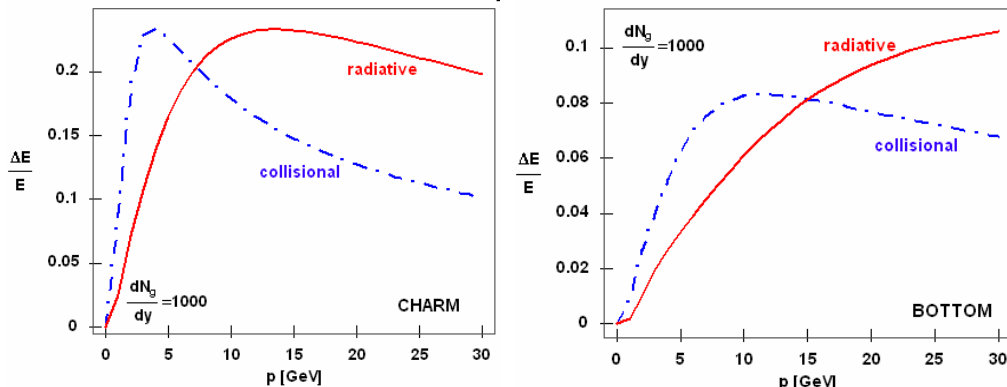


Figure 6: Comparison between collisional and medium induced radiative fractional energy loss is shown as a function of momentum for charm and bottom quark jets (left and right panels respectively). Full curves show the collisional energy loss, while dot-dashed curves show the net radiative energy loss. Assumed thickness of the medium is $L = 5$ fm and $\lambda = 1$ fm.

Comparison between collisional and medium induced radiative energy loss [33] is shown in Fig. 6. We see that collisional and medium induced radiative energy losses are comparable. Therefore, consistently with the claims in Refs. [26, 27], we see that collisional energy loss is important, and has to be included in the computation of jet quenching.

The results from Fig. 6 are still not included in the computation of jet quenching. However, in [17] we computed the single electron suppression by taking into account medium induced radiative energy loss together with two different computations (TG [29] and BT [30]) of collisional energy loss done in an infinite QCD medium (see Fig. 7). We see that with collisional energy loss, it is possible to reach single electron $R_{AA} \approx 0.5 \pm 0.1$ even at $dN_g/dy = 1000$. While the preliminary data suggest that $R_{AA} < 0.4$, these predictions are consistent with the data within present experimental and theoretical errors. Therefore, we may conclude that combined collisional and radiative pQCD approach may be able to solve a substantial part of the non-photon single electron puzzle.

We note that collisional energy loss in a finite size QCD medium falls between the two different computations [29, 30] used in [17] (for more details see [33]). Therefore, we expect that the single electron suppression results - computed with finite size collisional energy loss [33] - should be inside the middle yellow region presented in Fig. 7.

We also note that (see [16, 17]), any proposed solution of this puzzle must also be consistent with the extensive pion quenching data [1]. In [17] we show that the simultaneous inclusion of path fluctuations together with radiative and collisional energy loss makes it possible to satisfy $R_{AA}^e < 0.5 \pm 0.1$ without violating the bulk $dN_g/dy = 1000$ entropy constraint [5, 18] and without violating the pion quenching constraint $R_{AA}^{\pi^0} \approx 0.2 \pm 0.1$ now observed out to 20 GeV.

Finally, note that in this study we used constant coupling $\alpha_S = 0.3$. However, the radiative and elastic energy losses depend on the coupling, $\Delta E^{rad} \propto \alpha_S^3$ and $E^{el} \propto \alpha_S^2$. Future calculations will have to relax the current fixed α_S approximation and allow it to run. Additionally, the running coupling in collisional and radiative processes may be different, since these processes might probe different energy scales.

4 Conclusion

In this proceeding we applied the theory of heavy quark energy loss to non-photon single electron suppression. We showed that bottom quark contribution can not be neglected in the computation of

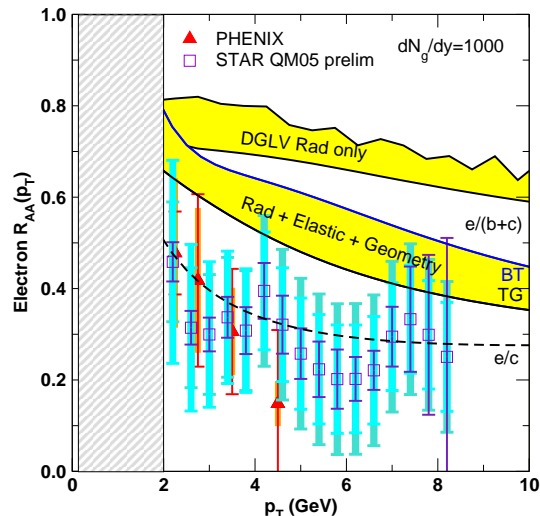


Figure 7: The suppression factor, $R_{AA}(p_{\perp})$, of non-photonic electrons from decay of quenched heavy quark ($c+b$) jets is compared to PHENIX [14] and preliminary STAR data [15] data in central Au+Au reactions at 200 AGeV. Assumed initial gluon rapidity density is $dN_g/dy = 1000$. The upper yellow band from [16] takes into account radiative energy loss only, using a fixed $L = 6$ fm; the lower yellow band includes both collisional and radiative energy losses as well as jet path length fluctuations [17]. The dashed curve shows the electron suppression using radiative and TG [29] collisional energy loss with bottom quark jets neglected. Figure adapted from [17].

single electron spectra. Additionally, we showed that the recent single electron data lead to significant discrepancies with theoretical predictions based only on radiative energy loss, as long as realistic values of gluon rapidity density are taken into account. Finally, we introduced the collisional energy loss mechanisms, and showed that combined collisional and radiative pQCD approach may be able to solve a substantial part of the non-photonic single electron puzzle.

Acknowledgments

I thank Miklos Gyulassy, Simon Wicks, William Horowitz and Ramona Vogt for the collaboration on the heavy quark energy loss projects. Valuable discussions with Ulrich Heinz are gratefully acknowledged. This work is supported by the U.S. Department of Energy, grant DE-FG02-01ER41190.

References

- [1] T. Isobe, arXiv:nucl-ex/0510085; M. Shimomura [PHENIX Collaboration], Nucl. Phys. A **774**, 457 (2006); S. S. Adler *et al.* [PHENIX Collaboration], Phys. Rev. Lett. **91**, 072301 (2003).
- [2] M. Gyulassy, I. Vitev, X. N. Wang and B. W. Zhang, Quark Gluon Plasma 3, (ed. R.C. Hwa and X.N. Wang, World Scientific, Singapore) pp. 123-191; A. Kovner and U. Wiedemann, pp. 192-248 *op cit.*; P. Jacobs and X. N. Wang, Prog. Part. Nucl. Phys. **54**, 443 (2005).
- [3] M. Gyulassy, P. Levai and I. Vitev, Phys. Lett. B **538**, 282 (2002).
- [4] I. Vitev and M. Gyulassy, Phys. Rev. Lett. **89**, 252301 (2002); X. N. Wang and M. Gyulassy, Phys. Rev. Lett. **68**, 1480 (1992).
- [5] M. Gyulassy and L. McLerran, Nucl. Phys. A **750**, 1 (2005).
- [6] N. Brambilla *et al.*, arXiv:hep-ph/0412158.

- [7] Yu. L. Dokshitzer and D. E. Kharzeev Phys. Lett. B **519**, 199 (2001).
- [8] M. Djordjevic and M. Gyulassy, Nucl. Phys. A **733**, 265 (2004).
- [9] M. Djordjevic and M. Gyulassy, Phys. Rev. C **68**, 034914 (2003); Phys. Lett. B **560**, 37 (2003).
- [10] M. Djordjevic, M. Gyulassy and S. Wicks, Phys. Rev. Lett. **94**, 112301 (2005); Eur. Phys. J. C **43**, 135 (2005).
- [11] B. W. Zhang, E. Wang and X. N. Wang, Phys. Rev. Lett. **93**, 072301 (2004).
- [12] N. Armesto, A. Dainese, C. A. Salgado and U. A. Wiedemann, Phys. Rev. D **71**, 054027 (2005).
- [13] J. W. Harris, arXiv:nucl-ex/0504023.
- [14] S. S. Adler [PHENIX Collaboration], Phys. Rev. Lett. **96**, 032301 (2006); Y. Akiba [PHENIX Collaboration], Nucl. Phys. A **774**, 403 (2006).
- [15] J. Bielcik [STAR Collaboration], Nucl. Phys. A **774**, 697 (2006). X. Dong, [STAR Collaboration], Nucl. Phys. A **774**, 343 (2006).
- [16] M. Djordjevic, M. Gyulassy, R. Vogt and S. Wicks, Phys. Lett. B **632**, 81 (2006).
- [17] S. Wicks, W. Horowitz, M. Djordjevic and M. Gyulassy, arXiv:nucl-th/0512076.
- [18] B. B. Back et al., Phys. Rev. Lett **88**, 022302 (2002).
- [19] M. Cacciari, P. Nason and R. Vogt, Phys. Rev. Lett. **95** 122001 (2005).
- [20] M. L. Mangano, P. Nason and G. Ridolfi, Nucl. Phys. B **373**, 295 (1992).
- [21] R. Vogt, Int. J. Mod. Phys. E **12**, 211 (2003).
- [22] B. Kampfer and O. P. Pavlenko, Phys. Lett. B **477**, 171 (2000).
- [23] B. G. Zakharov, JETP Lett. **76**, 201 (2002).
- [24] M. Djordjevic, Phys. Rev. C **73**, 044912 (2006).
- [25] R. Baier, Nucl. Phys. A **715**, 209 (2003).
- [26] M. G. Mustafa, Phys. Rev. C **72**, 014905 (2005); M. G. Mustafa and M. H. Thoma, Acta Phys. Hung. A **22**, 93 (2005).
- [27] A. K. Dutt-Mazumder, J. Alam, P. Roy and B. Sinha, Phys. Rev. D **71**, 094016 (2005).
- [28] J. D. Bjorken, FERMILAB-PUB-82-059-THY (unpublished).
- [29] M. H. Thoma and M. Gyulassy, Nucl. Phys. B **351**, 491 (1991).
- [30] E. Braaten and M. H. Thoma, Phys. Rev. D **44**, 2625 (1991).
- [31] X. N. Wang, M. Gyulassy and M. Plümer, Phys. Rev. D **51**, 3436 (1995); M. G. Mustafa, D. Pal, D. K. and M. Thoma, Phys. Lett. B **428**, 234 (1998); Z. Lin, R. Vogt and X. N. Wang, Phys. Rev. C **57**, 899 (1998).
- [32] S. Peigne, P. B. Gossiaux and T. Gousset, JHEP **0604**, 011 (2006).
- [33] M. Djordjevic, arXiv:nucl-th/0603066.